AD

AD-E400 697

TECHNICAL REPORT ARLCD-TR-81029

THEORETICAL AND EMPIRICAL EQUATIONS OF STATE
FOR NITROGEN GAS AT HIGH PRESSURE AND TEMPERATURE

THEODORE VLADIMIROFF

SEPTEMBER 1981

US ARMY ARMAMENT RESEARCH AND DEVELOPMENT COMMAND
LARGE CALIBER
WEAPON SYSTEMS LABORATORY
DOVER, NEW JERSEY

APPROVED FOR PUBLIC RELEASE; DISTRIBUTION UNLIMITED.

REPORT DOCUMENTATION PAGE		READ INSTRUCTIONS BEFORE COMPLETING FORM
1. REPORT NUMBER Technical Report ARLCD-TR-81029	2. GOVT ACCESSION NO.	3. RECIPIENT'S CATALOG NUMBER
4. TITLE *(and Subtitle)* THEORETICAL AND EMPIRICAL EQUATIONS OF STATE FOR NITROGEN GAS AT HIGH PRESSURE AND TEMPERATURE		5. TYPE OF REPORT & PERIOD COVERED 1977 through 1980
		6. PERFORMING ORG. REPORT NUMBER
7. AUTHOR(s) Theodore Vladimiroff		8. CONTRACT OR GRANT NUMBER(s)
9. PERFORMING ORGANIZATION NAME AND ADDRESS ARRADCOM, LCWSL Applied Sciences Div (DRDAR-LCA-G) Dover, NJ 07801		10. PROGRAM ELEMENT, PROJECT, TASK AREA & WORK UNIT NUMBERS
11. CONTROLLING OFFICE NAME AND ADDRESS ARRADCOM, TSD STINFO Div (DRDAR-TSS) Dover, NJ 07801		12. REPORT DATE September 1981
		13. NUMBER OF PAGES 41
14. MONITORING AGENCY NAME & ADDRESS*(If different from Controlling Office)*		15. SECURITY CLASS. *(of this report)* Unclassified
		15a. DECLASSIFICATION/DOWNGRADING SCHEDULE

16. DISTRIBUTION STATEMENT *(of this Report)*

Approved for public release; distribution unlimited.

17. DISTRIBUTION STATEMENT *(of the abstract entered in Block 20, if different from Report)*

18. SUPPLEMENTARY NOTES

19. KEY WORDS *(Continue on reverse side if necessary and identify by block number)*

Equations of state	Virial expansion	Ballistic calculations
Lennard-Jones	High temperature gas	
Percus-Yevic	High pressure gas	
Able-Noble	Thermodynamic properties	

20. ABSTRACT *(Continue on reverse side if necessary and identify by block number)*

Equations of state for nitrogen gas are investigated using both empirical and theoretical techniques. It was found that none of the empirical equations are accurate, thus seriously impairing the predictive capacity of current interior ballistic computer programs. Theoretical calculations which use a Lennard-Jones intermolecular potential in conjunction with the Percus-Yevic equation or the Verlet-Weis perturbation theory seem to be more accurate although the simple Lennard-Jones potential is not completely satisfactory. More realistic results

(cont)

DD FORM 1473 1 JAN 73   EDITION OF 1 NOV 65 IS OBSOLETE   UNCLASSIFIED

20. ABSTRACT (cont)

should be obtainable by use of the Maitland and Smith potential which allows more accurate pressure calculations for nitrogen as well as other propellant gases.

CONTENTS

TABLES

INTRODUCTION

One of the essential properties of a propellant is its burning rate which, unfortunately, has been poorly defined. Conceptually, there are various burning rates.

The strand burner gives a bulk burning rate at constant pressure but it may not reflect the rate at which the surface of individual propellant grains recedes, nor does it consider any interactive effects between grains or dynamic effects due to the variation of pressure.

A burning rate determined from a closed chamber firing should more closely reproduce the conditions actually encountered in a gun; however, current methods of evaluating burning rates from the pressure time trace do not yield the best parameters for use with ballistic codes. The same computer ballistic code should be used to evaluate the bomb data and to perform the ballistic calculation; that is, a closed bomb should be viewed as a gun with an infinite shot start pressure. In this way, the burning rate parameters obtained from the bomb will at least partially compensate for approximations made in the ballistic code and thus compensate for the same approximations made when calculating the muzzle velocity.

Finally the overall burning rate is determined by the slowest physical or chemical step. The faster processes cannot proceed until this slower step has been completed. The specific step cannot be identified at this time but it is probably in the gas phase. Otherwise, there would not be evidence of an exponential dependence of pressure on the burning rate.

In view of the importance of the burning rate in propellants and the fact that there are several phenomenological definitions of this quantity, an effort should be expended to clarify the conditions and to explain the discrepancies found in the different methods of measuring the burning rate. Part of this can be done experimentally; for example, by designing a bomb to burn a strand so that the method of calculating the burning rate from the pressure time trace can be checked. However, the rapid rate of combustion, as well as the high pressures and temperature, limit the amount of detailed knowledge that can be obtained from experiments. An alternative approach is to attempt a mathematical model of the ballistic combustion cycle. This approach seems more feasible because the laws of physics and chemistry are fairly well understood and modern electronic computers can be used to solve complicated equations which in the past were unsolvable. Several investigations have already been conducted and several computer ballistic codes are now available. There are the efforts of Kuo[1], Krier (ref 1), Gough (ref 2), and Fisher and Trippe (ref 3). These ballistic codes emphasize the gas dynamics of the flame's spreading but fail to consider the chemistry involved.

---

[1] Private communication, 1976.

1

The ballistic codes are based on an energy balance, the source of which is chemical in nature. The amount of energy released at any instant depends on the energy of the propellant consumed minus the energy of the products formed. The products formed depend on the pressure, the temperature, and the composition of the propellant gas. Thus, the temperature, pressure, and propellant gas composition must be accurately calculated at each step of the simulation. Calculating the temperature accurately requires knowing the heat capacity of the gas and the nature of the boundary layer which controls the heat flow out of the gun. The pressure must be accurately determined from the temperature and gas composition because it controls the burning rate and performs the work on the projectile. Thus, propellant gas composition becomes a vital consideration in an accurate model of interior ballistics. This composition is not considered in the models currently available.

Gas composition is also important for other reasons, the most prominent being muzzle flash and chemical erosion. It is widely believed that the most significant contribution to gun erosion is thermal; however, cool nitramine propellants have been considered and found to be more erosive than standard propellants with higher flame temperature. This could be due to the differences in the transport properties of the products or the presence in the propellant gas mixture of reactive molecules such as H_2, CO, O_2 which could be responsible for a chemical attack on the gun barrel. Changes in formulation can be sought to reduce the erosive species. Since muzzle flash is related to the presence of combustible gases at the muzzle, knowledge of the gas composition and temperature at each point of the ballistic cycle should allow prediction of the extent of flash for any composition.

Until now, gas composition has not been a factor in internal ballistic calculations because it has been difficult to include this type of consideration. However, developments in statistical mechanics and in the theory of simple fluids offer a resolution to this problem, providing the products of combustion are assumed to be in thermodynamic equilibrium. All propellants are inherently unstable substances and are in metastable equilibrium with their environment. The combustion of a propellant is not an equilibrium process, but if all rate processes are incorporated into the burning rate law, it may be fairly accurate to assume that the products of combustion are in thermodynamic equilibrium. This can be partially justified by estimating the number of collisions these molecules undergo in a short time compared to the ballistic cycle. A simple analysis is demonstrated in the appendix. Turbulence and pressure waves in the gun tube would also help maintain thermodynamic equilibrium between product molecules.

Thus, to obtain realistic values for the rate of propellant combustion, it is necessary to model the combustion process precisely. One of the most difficult aspects of this problem, even if thermodynamic equilibrium among products is assumed, is to obtain an accurate equation of state for a propellant gas mixture, mainly because there is no valid experimental data for a gas at 700 MPa and 3000°C. No container has been devised that will hold a gas at this temperature and at pressure long enough for a static measurement to be made. Dynamic types of measurements were made by Sandow (ref 4) by burning propellants in a closed bomb. In this experiment only the pressure was measured directly. A calculated flame temperature and a constant moles-of-gas-per-gram of propellant were used.

2

No effort was made to determine the extent of combustion or if chemical equilibrium had been established. Consequently, it became necessary to calculate the equation of state from theoretical considerations. Fortunately, the theory of simple fluids also yields the Gibbs free energy of the gas mixture which is necessary to calculate the equilibrium constants between propellant gas molecules such as the constant for the water-gas reaction. These constants are necessary as a function of pressure and temperature in order to calculate the propellant gas composition at each point in the ballistic cycle.

This report addresses the central problem of a good equation of state for a propellant gas. Some accurate experimental data (ref 5) were obtained on N_2 which is a typical propellant gas molecule. The data approach liquid densities and a maximum temperature of 1000°C, the limit set by conventional apparatus. The data are quoted to be accurate to 0.3%. For an estimate of the errors involved in using the equations of state currently employed in ballistic calculations, this data was fitted with empirical equations of state. Several theoretical methods based on an empirical intermolecular potential were also employed. Then the parameters in the empirical potential were adjusted to obtain the best fit of experimental data. Finally, the pressure of nitrogen at 3000 K was calculated.

COMPUTATIONAL DETAILS

Empirical equations of state were fitted to the nitrogen pressure data using the non-linear least-squares program of Moore and Zeigler (ref 6). This method uses the Newton-Raphson technique (ref 7) and requires that derivatives be calculated with respect to all adjustable parameters. The Percus-Yevic equation (ref 8) employs the direct correlation function $c(r)$:

$$G(r) = g(r)-1 = c(r) + \rho \int c(r')G(|r-r'|)dr$$

where $g(r)$ is the radial distribution function, with the approximation that

$$c(r) = g(r) \left\{ 1 - \exp [u(r)/k\,T] \right\} .$$

$u(r)$ is the intermolecular potential. k and T are defined in table 1. This equation was solved using a computer program[2] employing a method advocated first by Broyles (ref 9). It started with a trial solution g and was iterated until a self-consistent g was obtained. If the first input value of g is called "g_{in}" (old) and the result output value is called "g_{out}," then the second input, "g_{in}" (new) is given by:

---

[2] The program was supplied by Frederic Mandel, <u>Univ. of Cincinnati College of Medicine,</u> Dept. of Pharmacology and Cell Biophysics, Cincinnati, Ohio.

$$g_{in}(new) = \alpha\, g_{in}(old) + (1-\alpha)\, g_{out}$$

with $0 < \alpha < 1$. At high densities it is often necessary to use large values of α to achieve convergence.

The third virial coefficients were extrapolated from the tables compiled by Bird et al (ref. 10). Attempts to compute these values using modern methods of evaluating multidimensional integrals of Haselgrove (ref 11) and Conroy (ref 12), were unsuccessful because of inaccuracies in the methods. A computer program to perform the Verlet-Weis perturbation theory (ref 13) was then written. A least-squares computer program which does not use derivatives was used in order to adjust the Lennard-Jones potential for the best fit of nitrogen pressure data. This technique was programmed incorporating Powell's ideas (ref 14) concerning the variation of parameters along conjugate directions.

RESULTS AND DISCUSSION

In the investigation of the role of the equation of state in propellant combustion, the pressure-volume-temperature data of Malbrunot and Vodar (ref 5) was used. These data, stated to be accurate to 0.3%, span the temperature range of 200°C to 1000°C and 0.1618 g/cm^3 to 0.8222 g/cm^3 in density. These data were fit to popularly-used equations of state at various temperatures to ascertain the degree of accuracy of the equations of state currently employed in interior ballistic calculations. The data at 600°C were excluded because of obvious errors. Consideration was given to the virial expansion using just the second virial coefficient as employed in the Calspan code (ref 3), the Able-Noble equation which is used by other ballisticians, and two virial coefficients as used in the BLAKE code (ref 15). Also tried was an equation of state which had recently been found to be very accurate for hard spheres (ref 16). The functional form of the equations is summarized in table 1. Tables 2 through 9 record the calculated results, the experimental values of Malbrunot and Vodar, and the errors reported as a percentage of the experimental values. It was evident that the need exists for a simple, accurate equation of state that can be used in ballistic calculations as well as a method which will becomes more accurate as temperatures increase. Since there is no experimental data at 3000 K, a search should be made for a simple method for extrapolating to high temperature.

Calculations in tables 2 through 9 showed that none of the simple methods works well. The Able-Noble equation was particularly disappointing. This approach worked at 200°C, but as temperature increased, agreement with the experiment steadily became worse, until at 1000°C there were 9% errors. This is under the best situation where the covolume was allowed to be a function of temperature (covolume increased with temperature). Usually the covolume is assumed to be a constant, and in this case errors as great as 15% can be encountered. In a realistic computer model, errors of this magnitude cannot be tolerated. To obtain reasonable results, it is necessary to adjust "shot-start" pressure, burning rate parameters, and heat losses.

Keeping only the "second" virial coefficient is also a very poor approximation although this approach improves with temperature. Using the "second" and "third" virial coefficients gives the best results, but large increases of the

4

"third" virial coefficient with temperature make any attempt at extrapolation to 3000 K questionable. The use of the equation of state which is known to be accurate for hard spheres seems to yield readily to physical interpretation. This equation gives poor results at 200°C where the attractive part of the potential is still important. As temperature increases, these attractive forces are more easily overwhelmed and the N_2 molecules start to behave like hard spheres. Also, the effective hard-sphere volume decreases as a function of temperature. When plotted as a function of the reciprocal of the absolute temperature, it extrapolates smoothly to a value which can be used at 3000 K. This extrapolation is depicted in figure 1.

Because of the rather poor performance of the empirical equations of state, the theories of simple fluids were applied to calculate the pressure of nitrogen gas and compare the calculated values to the experimental data. These methods employ an intermolecular potential function. The Percus-Yevic method calculates thermodynamic properties in terms of the two-particle distribution function. The perturbation theory of Verlet-Weis and the more conventional virial expansion were used to calculate thermodynamic properties directly. The virial expansion is exact and becomes approximate because only the second and third virial coefficients were used. Results of computations employing the Lennard-Jones potential

$$u(r) = 4\varepsilon\left[\left(\frac{\sigma}{r}\right)^{12} - \left(\frac{\sigma}{r}\right)^{6}\right]$$

are shown in tables 10 through 17. In this study,

$$\sigma = 0.3698 \text{ nm and } \frac{\sigma}{k} = 95.05 \text{ K for } N_2.$$

Several conclusions can be made on the basis of these calculations. The most accurate pressures were obtained with the Percus-Yevic equation. The greatest deviation was 7.6% at low temperature and high density. The Verlet-Weis theory was less accurate. Since all the methods improve with increasing temperature, the pressure of nitrogen was computed at 3000 K. The results of these calculations are recorded in table 18 and compared with extrapolated values obtained using the hard-sphere equation of state. Good agreement was obtained with the Percus-Yevic equation. The agreement was reduced when the Verlet-Weis perturbation theory was employed. (The two-term virial equation is always too low because higher order virial coefficients are not used.)

For accurate interior ballistic calculations, agreement of several percent is inadequate. Good agreement between the Percus-Yevic and the Verlet-Weis theories indicated that the discrepancies were probably due to the fact that the Lennard-Jones potential did not accurately describe the nitrogen intermolecular potential. Since the σ and the ε are numbers obtained by fitting experimental data, these quantities were adjusted to obtain the best fit of the experimental nitrogen pressures. The Percus-Yevic theory is computationally too complex for this type of effort, but the Verlet-Weis theory requires little computer time and is easily adapted to this type of approach. The deviation between experimental and calculated points is some function of σ and ε; however, this function is complex and there does not seem to be any simple way to calculate derivatives with respect to σ and ε. For this reason, the Powell method was used which requires no derivatives to minimize the deviation with respect to σ and ε. The
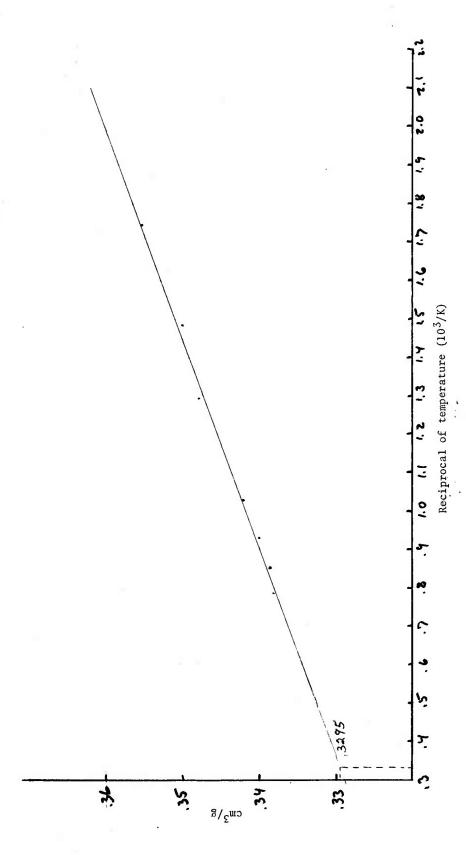
Figure 1. Extrapolation of "hard-sphere" volume of nitrogen to T = 3000 K

best values of σ and ε were obtained for each temperature; results are shown in table 19.

The calculations fall into two categories. In the temperature range from 200°C to 600°C, good agreement is obtained and the distortion of the potential is small. At elevated temperatures, the agreement is poor and distortion of the Lennard-Jones potential is much greater. This illustrates a well-known inadequacy of the Lennard-Jones potential; i.e., the repulsive part is too steep. At high temperatures, the attractive part is not very important and the ε can be adjusted to obtain a more realistic repulsive potential, although not very successfully. To remedy this problem a more realistic potential is required. A modified version of the Lennard-Jones 6-12 potential has been suggested by Maitland and Smith (ref 17):

$$u(r*) = \varepsilon \left[\left(\frac{6}{n-6} \right) (r*)^{-m} - \left(\frac{m}{m-6} \right) (r*)^{-6} \right],$$

$$m = 13 + \gamma (r*-1),$$

where $r* = r/r_{min}$ and r_{min} is the separation at the minimum energy, $-\varepsilon$. This potential is of the Lennard-Jones 6-12 type if m is set equal to 12. A more flexible and realistic potential is achieved by allowing the m to vary with intermolecular distance. Aziz (ref 18) found that if this potential is applied to neon, the parameters ε, r_{min}, and γ can be evaluated from three dilute gas bulk properties; thermal diffusion, viscosity, and second virial coefficients. The resulting potential predicts not only dilute gas bulk properties but also spectroscopic and molecular beam data as well as much more complex realistic potentials (ref 17). This new potential could yield accurate pressure determinations for propellant gases at high temperature.

CONCLUSIONS

The simple equations of state usually employed in ballistic-type calculations such as the Able-Noble equation and the two-term virial expansion are not accurate. The virial expansion is better for ballistic calculations since it improves with temperature, but it is not amenable to accurate extrapolations. On the other hand, modern theories of fluids such as the Percus-Yevic theory and the perturbation theory of Verlet-Weis offer a reasonable method of determining an equation of state for propellant gases at high temperature and pressure, with the best results being consistently obtained with the Percus-Yevic equation. The Lennard-Jones intermolecular potential is not flexible enough for description of nitrogen-nitrogen interactions at high temperatures.

RECOMMENDATIONS

Because of the poor performance of the equations of state used in conventional ballistic codes and the total lack of consideration of the propellant gas composition, there may be merit in combining the BLAKE thermodynamic code with an interior ballistic code. This combination would permit calculation of the gas composition at each point in the ballistic cycle and would provide an equation of state based on a two-term virial expansion which is more accurate than the equation of state presently employed. Such a program could be combined with a least-squares technique to obtain burning rate data from a closed bomb pressure time trace, the burning rate parameters being adjusted until the best least-squares fit of the pressure time trace is obtained.

The new molecular interaction potential of Maitland and Smith should be utilized to get a more accurate pressure calculation for nitrogen as well as other propellant gases. This could result in calculations of more accurate thermodynamic properties of propellant gas mixtures.

The experimental data obtained by Malbrunot and Vodar for nitrogen did not include pressure information above 1000°C, but it proved helpful in this study. Similar experimental pressure data should be obtained, collectively and separately, on other propellant gas molecules such as CO, H_2, H_2O, CO_2, N_2, and CH_4.

REFERENCES

1. H. Krier and M. J. Adams, "Predicting Uniform Gun Interior Ballistics, Part II, The Interior Ballistic Code," University of Illinois Technical Report AAE 74-6, Urbana, IL, 1974.

2. P. S. Gough, "Fundamental Investigation of the Interior Ballistics of Guns," Indian Head Contract Report 74-1, Indian Head, MD, 1974.

3. E. B. Fisher and A. P. Trippe, "Development of Basis for Acceptance of Continuously Produced Propellant," Calspan Report VQ-5163-D-1, Calspan Corp., Buffalo, NY, 1973.

4. J. Sandow, "High Pressure Combustion Study of a Double-Base Propellant," PA Technical Memorandum 1953, Picatinny Arsenal, Dover, NJ, 1970.

5. P. Malbrunot and B. Vodar, "Experimental pVT Data and Thermodynamic Properties of Nitrogen up to 1000°C and 5000 Bar," Physica, vol 66, 1973, p 351.

6. R. H. Moore and R. R. Zeigler, "The Solution of the General Least Squares Problem with Special Reference to High Speed Computers," Los Alamos Report 2367, Los Alamos Scientific Lab., Los Alamos, NM, 1960.

7. C. T. Fike, Computer Evaluation of Mathematical Functions, Prentice-Hall, Inc., Englewood Cliffs, NY, 1968, p 23.

8. J. K. Percus and G. J. Yevic, "Analysis of Classical Statistical Mechanics by Means of Collective Coordinates," Phys. Rev., vol 110, 1958, p 1.

9. A. A. Broyles, "Solutions of the Percus-Yevick Equation," J. Chem. Phys., vol 35, 1961, p 493.

10. R. B. Bird, E. L. Spotz, and J. O. Hirschfelder, "The Third Virial Coefficient for Non-Polar Gases," J. Chem. Phys., vol 18, 1950, p 1395.

11. C. B. Haselgrove, "A Method for Numerical Integration," Math. Computation, vol 15, 1961, p 323.

12. H. Conroy, "Molecular Schrodinger Equation VIII. A New Method for the Evaluation of Multidimensional Integrals," J. Chem. Phys., vol 47, 1967, p 5307.

13. L. Verlet and J. J. Weis, "Equilibrium Theory of Simple Liquids," Phys. Rev., vol 5A, 1972, p 939.

14. M. J. D. Powell, "An Efficient Method for Finding the Minimum of a Function of Several Variables without Calculating Derivates," Comp J., vol 7, 1964, p 155.

15. E. Freedom, "A Brief Users' Guide for the BLAKE Program," BRL Interim Memorandum Report 249, Ballistic Research Labs., Edgewood Arsenal, Aberdeen Proving Ground, MD, 1974.

16. N. F. Carnahan and K. E. Starling, "Equation of State for Nonattracting Rigid Spheres," J. Chem. Phys., vol 51, 1969, p 635.

17. G. C. Maitland and E. B. Smith, "A Simplified Representation of Intermolecular Potential Energy," Chem. Phys. Lett., vol 22, 1973, p 443.

18. A. Aziz, "A New Realistic Potential for Neon Based on Dilute Gas Bulk Properties, Chem. Phys. Lett., vol 40, 1976, p 57.

APPENDIX

PARTIAL JUSTIFICATION OF CHEMICAL EQUILIBRIUM OF PROPELLANT GASES

For achievement of chemical equilibrium in a propellant gas during the ballistic event, several criteria must be met. There should be sufficient collisions to give individual molecules a chance to react with each other in a short time compared to the total ballistic cycle. The temperature should be high enough for chemical reaction; that is, the temperature should be above the "freeze-out" temperature. Since at high density, mean-free paths of molecules may be quite short, mixing of propellant gas molecules may be very slow. It is therefore vital that the contents of the chamber be inherently homogeneous.

For estimating the number of collisions in a mixture of propellant gases, formula for the number of collisions, f was used:

$$f = \pi \, d^2 n \, \sqrt{2} \, v$$

where d is the diameter of the molecule, v is its velocity and n is the number density. For a typical molecule at room temperature, d is 2.25×10^{-8} cm, and the velocity is 10^5 cm/sec. At 100 KPa of pressure, there are about 3×10^{19} molecules/cm^3. Substitution of these values in the above formula resulted in 7×10^9 collisions per second. If the time for the ballistic cycle is taken as 10 milliseconds and the total is divided into 10^4 steps for the purpose of numerical integration, in each of the small-time intervals there are 7×10^3 collisions. There should be sufficient collisions to maintain chemical equilibrium. At increased temperature and pressure (as is actually experienced in the gun environment), both v and n increase so that even more collisions occur to maintain chemical equilibrium.

Freeze-out temperature for a propellant is about 1000 K while the flame temperature is over 2000 K, so that there should be sufficient energy in an average collision to insure the possibility of chemical reaction and the maintenance of chemical equilibrium. Because mean-free paths of propellant gas molecules may be quite short at high densities, mixing may be very slow between different regions. However, if the propellant is homogeneous and the products of combustion are the same in all parts of the chamber, extensive mixing should not be necessary. Any turbulence of pressure waves that travel in the combustion chamber will, of course, promote mixing if it is required.

13

Table 1. Empirical and theoretical equations of state
currently employed in propellant calculations

Able-Noble

$$p = \rho k \, T(1-y)^{-1}$$

Virial Expansion*

$$p = \rho kT(1 + B_2(T) \, \rho + B_3(T)\rho^2 + \ldots.$$

Hard Sphere

$$p = \rho kT(1 + y + y^2 - y^3)(1 - y)^{-3}$$

ρ = gas density (g/cm^3)

b = adjustable parameter (cm^3/g)

y = ρb

k = Baltzman constant $(MPa \; cm^3/g \; K)$

P = pressure (MPa)

T = temperature (K)

---

* This equation can be either empirical or theoretical depending on whether B(T)'s are determined from experimental data or calculated from an intermolecular potential as employed in BLAKE.

Table 2. Observed and calculated pressure of nitrogen
at 200°C using empirical equations of state

				Calculated					
Density (g/cm³)	Observed* (MPa)	Able-Noble (MPa)	Error (%)	One virial coefficient (MPa)	Error (%)	Two virial coefficients (MPa)	Error (%)	Hard sphere (MPa)	Error (%)
0.3661	75.88	78.68	-3.7	109.18	-43.9	71.22	6.1	91.03	-20.0
0.4247	99.73	99.74	0.0	137.38	-37.7	95.36	4.3	116.47	-16.8
0.5082	141.5	137.5	2.8	182.69	-29.1	141.0	3.3	160.8	-13.6
0.5691	180.7	173.3	4.1	219.52	-21.5	184.2	-1.9	200.3	-10.8
0.6194	221.3	210.3	4.9	252.3	-14.0	227.1	-2.6	238.4	-7.7
0.6642	265.12	251.3	5.2	283.4	-6.9	271.3	-2.3	277.2	-4.6
0.6970	302.14	287.78	4.8	307.3	-1.7	307.6	-1.8	309.0	-2.3
0.7250	337.1	324.6	3.7	328.4	2.6	341.4	-1.3	338.5	-4.2
0.7423	360.4	350.7	2.7	341.7	5.9	363.6	-0.9	358.0	0.7
0.7689	399.6	396.9	0.7	362.8	9.2	399.7	0.0	389.8	2.4
0.7708	402.6	400.5	0.5	364.3	9.5	402.4	0.0	392.2	2.6
0.8007	453.7	464.8	-2.4	388.9	14.3	446.3	1.6	431.3	4.9
0.8222	494.2	521.1	-5.4	406.8	17.7	480.0	2.8	461.6	6.6

* Experimental data taken from P. Malbrunot and B. Vodar, "Experimental pVT Data and Thermodynamic Properties of Nitrogen up to 1000°C and 5000 Bar," Physica, vol 66, 1973, p 351.

Table 3. Observed and calculated pressure of nitrogen at 300°C using empirical equations of state

Calculated

Density (g/cm³)	Observed* (MPa)	Able-Noble (MPa)	Error (%)	One virial coefficient (MPa)	Error (%)	Two virial coefficients (MPa)	Error (%)	Hard sphere (MPa)	Error (%)
0.36532	98.4	95.8	2.6	123.5	-25.5	94.2	4.3	107.9	-9.7
0.3824	106.2	102.9	3.1	132.3	-24.5	102.2	3.8	116.1	-9.3
0.41644	122.7	118.2	3.7	150.6	-22.7	119.7	2.4	133.6	-8.9
0.45213	141.7	136.1	3.9	170.9	-20.6	140.5	0.9	153.8	-8.5
0.51124	178.4	171.2	4.0	207.1	-16.1	180.8	-1.4	191.8	-7.5
0.5362	196.5	188.4	4.1	223.4	-13.7	200.3	-2.0	209.8	-6.8
0.57164	225.6	216.1	4.2	247.4	-9.7	230.7	-2.3	237.5	-5.3
0.6108	263.0	252.0	4.2	275.4	-4.7	268.2	-2.0	271.4	-3.2
0.63276	286.4	275.2	3.9	291.7	-1.8	291.1	-1.6	292.1	-2.0
0.65982	317.5	307.4	3.2	312.4	1.6	321.4	-1.3	319.3	-0.6
0.68887	353.7	347.6	1.7	335.3	5.2	356.4	-0.8	350.9	0.8
0.70971	382.0	380.8	0.3	352.2	7.8	383.2	-0.3	375.2	1.8
0.72954	411.7	416.5	-1.2	368.7	10.4	410.1	0.4	399.6	2.9
0.74125	431.0	439.8	-2.0	378.6	12.1	426.6	1.0	414.7	3.8
0.76889	480.7	502.8	-4.6	402.5	16.2	467.4	2.8	452.2	5.9

* Experimental data taken from P. Malbrunot and B. Vodar, "Experimental pVT Data and Thermodynamic Properties of Nitrogen up to 1000°C and 5000 Bar," Physica, vol 66, 1973, p 351.

Table 4. Observed and calculated pressure of nitrogen at 400°C using empirical equations of state

Density (g/cm³)	Observed* (MPa)	Calculated							
		Able-Noble (MPa)	Error (%)	One virial coefficient (MPa)	Error (%)	Two virial coefficients (MPa)	Error (%)	Hard sphere (MPa)	Error (%)
0.30735	89.51	87.67	2.0	109.33	-22.1	86.51	3.3	96.64	-8.0
0.3422	106.0	102.59	3.2	127.78	-20.5	102.87	2.9	113.60	-7.2
0.37162	121.0	116.42	3.8	144.31	-19.3	118.30	2.2	129.20	-6.8
0.41663	146.3	140.16	4.2	171.30	-17.1	145.08	0.8	155.60	-6.4
0.46731	179.15	171.48	4.3	204.16	-14.0	180.34	-0.7	189.40	-5.7
0.5103	211.82	202.88	4.2	234.07	-10.5	214.93	-1.5	221.89	-4.7
0.5325	230.85	221.23	4.2	250.25	-8.4	234.62	-1.6	240.20	-4.0
0.57234	269.3	258.7	3.9	280.5	-4.2	273.3	-1.4	275.9	-2.5
0.58405	281.7	271.0	3.8	289.8	-2.8	285.5	-1.4	287.2	-1.9
0.6103	311.3	301.0	3.3	310.9	0.1	314.4	-1.0	313.7	-0.8
0.63181	337.3	328.7	2.6	328.8	2.5	339.6	-0.7	336.9	0.1
0.65847	371.7	367.4	1.2	351.5	5.4	372.9	-0.3	367.6	1.1
0.68986	416.0	420.9	-1.2	379.3	8.8	415.0	0.2	406.6	2.2
0.71065	449.0	462.2	-2.9	398.2	11.3	444.9	0.9	434.4	3.2
0.72872	481.3	502.8	-4.4	415.0	13.8	472.0	1.9	459.9	4.4

* Experimental data taken from P. Malbrunot and B. Vodar, "Experimental pVT Data and Thermodynamic Properties of Nitrogen up to 1000°C and 5000 Bar," Physica, vol 66, 1973, p 351.

17

Table 5. Observed and calculated pressure of nitrogen at 500°C using empirical equations of state

Density (g/cm^3)	Observed* (MPa)	Calculated							
		Able–Noble (MPa)	Error (%)	One virial coefficient (MPa)	Error (%)	Two virial coefficients (MPa)	Error (%)	Hard sphere (MPa)	Error (%)
0.26306	82.5	81.71	1.0	98.59	-19.5	81.58	1.1	88.49	-7.3
0.29259	97.15	94.64	2.6	114.43	-17.8	95.48	1.7	102.95	-6.0
0.34255	124.5	119.13	4.3	143.43	-15.2	122.30	1.8	130.18	-4.5
0.3715	142.0	135.08	4.9	161.49	-13.7	139.94	1.4	147.70	-4.0
0.41637	171.85	162.91	5.2	191.32	-11.3	170.68	0.7	177.68	-3.4
0.46767	210.6	200.39	4.8	228.14	-8.3	211.39	-0.4	216.64	-2.9
0.51182	248.73	238.86	4.0	262.16	-5.4	251.66	-1.2	254.71	-2.4
0.5313	267.3	258.1	3.4	277.9	-4.0	271.1	-1.4	273.0	-2.1
0.55406	290.7	282.7	2.8	296.7	-2.1	295.1	-1.5	295.6	-1.7
0.5721	310.8	304.0	2.2	312.1	0.4	315.3	-1.4	314.5	-1.2
0.61041	359.1	355.7	0.9	345.9	3.7	361.4	0.6	357.8	-0.4
0.63209	390.0	389.7	0.1	365.8	6.2	389.5	1.3	384.3	1.4
0.65854	430.0	436.8	-1.5	390.7	9.1	425.9	0.9	418.8	2.6
0.6901	480.2	503.3	-4.8	421.4	12.2	472.6	1.6	463.4	3.5

* Experimental data taken from P. Malbrunot and B. Vodar, "Experimental pVT Data and Thermodynamic Properties of Nitrogen up to 1000°C and 5000 Bar," Physica, vol 66, 1973, p 351.

Table 6. Observed and calculated pressure of nitrogen at 700°C using empirical equations of state

					Calculated				
Density (g/cm^3)	Observed* (MPa)	Able-Noble (MPa)	Error (%)	One virial coefficient (MPa)	Error (%)	Two virial coefficients (MPa)	Error (%)	Hard sphere (MPa)	Error (%)
0.23976	94.8	91.25	3.7	106.79	-12.6	95.45	-0.7	97.43	-2.8
0.28552	123.0	115.68	5.9	135.70	-10.3	122.24	0.6	124.21	-1.0
0.31924	145.6	135.81	6.7	158.76	-9.0	144.35	0.8	146.12	-0.4
0.34213	161.9	150.66	6.9	175.26	-8.2	160.59	0.8	162.14	-0.1
0.36997	182.85	170.19	6.9	196.24	-7.3	181.78	0.6	182.97	-0.1
0.41611	220.6	206.69	6.3	233.26	-5.7	220.58	0.0	221.03	-0.2
0.46171	262.3	248.99	5.1	272.57	-3.9	263.79	-0.6	263.44	-0.4
0.49141	292.4	280.7	4.0	299.6	-2.5	294.7	-0.8	293.9	-0.5
0.53231	338.7	330.9	2.3	338.8	0.0	341.2	-0.7	340.0	-0.4
0.56183	376.1	373.2	0.8	368.4	2.0	377.6	-0.4	376.4	-0.1
0.58396	406.2	408.8	-0.6	391.4	3.6	406.6	-0.1	405.6	0.1
0.60891	442.0	453.8	-2.7	418.0	5.4	441.1	0.2	440.7	0.3
0.63278	480.1	502.8	-4.7	444.2	7.5	476.0	0.9	476.5	0.8

* Experimental data taken from P. Malbrunot and B. Vodar, "Experimental pVT Data and Thermodynamic Properties of Nitrogen up to 1000°C and 5000 Bar," Physica, vol 66, 1973, p 351.

Table 7. Observed and calculated pressure of nitrogen
at 800°C using empirical equations of state

| | | | | Calculated | | | | | |
Density (g/cm³)	Observed* (MPa)	Able-Noble (MPa)	Error (%)	One virial coefficient (MPa)	Error (%)	Two virial coefficients (MPa)	Error (%)	Hard sphere (MPa)	Error (%)
0.2037	84.25	81.78	2.9	93.88	-11.4	85.77	-1.8	86.41	-2.6
0.2484	111.55	105.78	5.2	122.25	-9.6	112.00	-0.4	112.49	-0.8
0.2863	137.62	128.52	6.6	148.49	-7.9	136.92	0.5	137.13	0.4
0.3196	162.65	150.65	7.4	173.20	-6.5	161.02	1.0	160.91	1.1
0.3414	180.0	166.4	7.6	190.2	-5.7	178.0	1.1	177.6	1.3
0.3800	212.4	197.0	7.2	222.0	-4.5	210.5	0.9	209.7	1.3
0.4152	243.7	228.5	6.2	252.8	-3.7	243.1	0.2	241.9	0.8
0.4621	289.2	277.1	4.2	296.5	-2.5	291.1	-0.6	289.6	-0.1
0.4917	321.2	312.6	2.7	325.6	-1.4	324.2	-0.9	322.8	-0.5
0.5194	354.6	349.8	1.4	354.0	0.2	357.4	-0.8	356.4	-0.5
0.5343	374.1	371.7	0.6	369.8	1.2	376.1	-0.5	375.4	-0.4
0.5601	410.0	413.3	-0.8	397.7	3.0	410.1	0.0	410.3	-0.1
0.5833	443.3	455.3	-2.7	423.6	4.4	442.2	0.2	443.6	-0.1
0.6099	485.3	509.7	-5.0	454.3	6.4	481.2	0.8	484.5	1.7

Table 8. Observed and calculated pressure of nitrogen
at 900°C using empirical equations of state

Density (g/cm³)	Observed* (MPa)	Calculated							
		Able-Noble (MPa)	Error (%)	One virial coefficient (MPa)	Error (%)	Two virial coefficients (MPa)	Error (%)	Hard sphere (MPa)	Error (%)
0.2009	92.3	88.08	4.6	99.98	-8.3	93.89	-1.7	92.67	-0.4
0.2521	126.44	118.35	6.5	135.06	-6.6	127.24	-0.5	125.29	1.1
0.2863	153.0	141.1	7.8	160.7	-5.0	152.1	0.6	149.6	2.2
0.3177	179.1	164.0	8.4	185.7	-3.7	176.9	1.2	174.0	2.8
0.3400	198.3	181.7	8.4	204.4	-3.1	195.7	1.3	192.6	2.9
0.3798	233.7	216.5	7.4	239.6	-2.5	231.8	0.8	228.5	2.2
0.4161	267.5	252.6	5.6	273.7	-2.3	267.8	-0.1	264.6	1.1
0.4372	288.4	275.8	4.4	294.4	-2.1	290.1	-0.6	287.3	0.4
0.4630	315.8	306.8	2.9	320.7	-1.5	318.9	-1.0	316.7	-0.3
0.4915	349.4	344.8	1.3	350.9	-0.4	352.5	-0.9	351.5	-0.6
0.5090	372.2	370.5	0.5	370.0	-0.6	374.2	-0.5	374.3	-0.6
0.5334	406.2	409.6	0.8	397.4	2.2	405.8	0.1	407.7	-0.4

* Experimental data taken from P. Malbrunot and B. Vodar, "Experimental pVT Data and Thermodynamic Properties of Nitrogen up to 1000°C and 5000 Bar," Physica, vol 66, 1973, p 351.

Table 9. Observed and calculated pressure of nitrogen
at 1000°C using empirical equations of state

				Calculated					
Density (g/cm³)	Observed* (MPa)	Able-Noble (MPa)	Error (%)	One virial coefficient (MPa)	Error (%)	Two virial coefficients (MPa)	Error (%)	Hard sphere (MPa)	Error (%)
0.1618	78.5	73.41	6.5	81.91	-4.3	78.59	-0.1	76.54	2.9
0.1774	87.75	82.08	6.4	92.01	-4.8	88.22	-0.5	85.81	2.2
0.2041	105.02	97.74	6.9	110.18	-4.9	105.63	-0.6	102.59	2.3
0.2439	134.07	123.22	8.1	139.37	-3.9	133.87	0.1	129.89	3.1
0.3173	196.06	178.41	9.0	199.80	-1.9	193.61	1.2	188.33	3.9
0.3407	217.2	198.7	8.5	220.9	-1.6	214.9	1.1	209.43	3.6
0.3803	254.3	236.8	6.9	258.5	-1.6	253.4	0.3	248.20	2.4
0.4172	291.1	277.2	4.8	295.8	-1.6	292.4	-0.4	288.1	1.0
0.4374	312.75	301.7	3.5	317.1	-1.4	315.0	-0.7	311.6	0.4
0.4613	340.3	333.2	2.1	343.2	-0.8	343.0	-0.8	341.0	-0.2
0.4905	377.4	376.0	3.8	376.3	0.3	379.1	-0.4	379.6	-0.6
0.5076	400.7	403.5	-7.1	396.3	1.1	401.1	-0.1	403.5	-0.7
0.5351	439.2	452.5	3.0	429.4	2.2	438.1	0.2	444.4	-1.2
0.5628	480.3	508.4	-5.9	464.0	3.4	477.4	0.6	488.5	-1.7

* Experimental data taken from P. Malbrunot and B. Vodar, "Experimental pVT Data and Thermodynamic
Properties of Nitrogen up to 1000°C and 5000 Bar," Physica, vol 66, 1973, p 351.

Table 10. Observed and calculated pressure of nitrogen at 200°C
using the Lennard-Jones 6-12 intermolecular potential

Density (g/cm³)	Observed* (MPa)	Calculated					
		Percus-Yevic (MPa)	Error (%)	Verlet-Weis (MPa)	Error (%)	Two virial coefficients (MPa)	Error (%)
0.3661	75.88	79.43	4.7	79.19	4.4	73.01	-3.8
0.4247	99.73	103.37	3.6	103.33	3.6	91.14	-8.6
0.5082	141.5	148.3	4.8	147.57	4.3	121.42	-14.2
0.5691	180.7	191.6	6.0	192.6	6.6	147.2	-18.5
0.6194	221.3	236.0	6.6	242.8	9.7	171.1	-22.7
0.6642	265.12	283.3	6.8	290.87	9.7	194.6	-26.6
0.697	302.14	323.3	7.0	334.95	10.8	213.1	-29.5
0.725	337.1	361.5	7.2	377.6	12.0	229.8	-31.8
0.7423	360.4	387.2	7.4	411.9	14.3	240.6	-33.2
0.7689	399.6	429.9	7.6	461.0	15.4	257.9	-35.5
0.7708	402.6	433.1	7.6	464.7	15.4	259.2	-35.6
0.8007	453.7	486.1	7.1	527.0	16.2	279.7	-38.4
0.8222	494.2	528.2	6.8	568.9	15.1	295.2	-40.3

* Experimental data taken from P. Malbrunot and B. Vodar, "Experimental pVT Data and Thermodynamic
Properties of Nitrogen up to 1000°C and 5000 Bar," Physica, vol 66, 1973, p 351.

23

Table 11. Observed and calculated pressure of nitrogen at 300°C using the Lennard-Jones 6-12 intermolecular potential

		Calculated					
Density (g/cm^3)	Observed* (MPa)	Percus-Yevic (MPa)	Error (%)	Verlet-Weis (MPa)	Error (%)	Two virial coefficients (MPa)	Error (%)
0.36532	98.4	99.2	0.8	99.3	0.9	92.2	-6.3
0.3824	106.2	105.7	0.5	107.3	1.0	98.6	-7.2
0.41644	122.7	124.6	1.5	125.0	1.9	112.2	-8.6
0.45213	141.7	145.3	2.5	146.2	3.2	127.7	-9.9
0.51124	178.4	186.1	4.3	188.7	5.8	156.1	-12.5
0.5362	196.5	206.2	4.9	209.8	6.8	169.2	-13.9
0.57164	225.6	238.0	5.5	243.6	7.8	189.0	-16.2
0.6108	263.0	278.2	5.8	287.0	9.1	212.6	-19.2
0.63276	286.4	303.4	5.9	314.5	9.8	226.7	-20.8
0.65982	317.5	337.3	6.2	351.8	10.8	244.9	-22.9
0.68887	353.7	377.4	6.7	396.5	12.1	265.6	-24.9
0.70971	382.0	408.8	7.0	431.9	13.1	281.0	-26.4
0.72954	411.7	440.9	7.1	468.2	13.7	296.4	-28.0
0.74125	431.0	460.9	6.9	491.1	13.9	305.7	-29.1
0.76889	480.7	511.4	6.4	542.0	12.7	328.5	-31.7

* Experimental data taken from P. Malbrunot and B. Vodar, "Experimental pVT Data and Thermodynamic Properties of Nitrogen up to 1000°C and 5000 Bar," Physica, vol 66, 1973, p 351.

Table 12. Observed and calculated pressure of nitrogen at 400°C using the Lennard-Jones 6-12 intermolecular potential

		Calculated					
Density (g/cm³)	Observed* (MPa)	Percus-Yevic (MPa)	Error (%)	Verlet-Weis (MPa)	Error (%)	Two virial coefficients (MPa)	Error (%)
0.30735	89.51	90.41	1.0	89.34	-0.2	86.78	-3.0
0.3422	106.0	106.82	0.8	107.06	1.6	101.1	-4.6
0.37162	121.0	122.2	1.0	122.67	1.4	114.1	-5.7
0.41663	146.3	149.0	1.8	149.98	2.5	135.8	-7.2
0.46731	179.15	184.6	3.0	186.67	4.2	162.9	-9.1
0.5103	211.82	220.1	3.9	223.75	5.6	188.4	-11.0
0.5325	230.85	240.6	4.2	245.39	6.3	202.5	-12.3
0.57234	269.3	281.7	4.6	289.1	7.3	229.4	-14.8
0.58405	281.7	294.8	4.6	303.3	7.7	237.8	-15.6
0.6103	311.3	326.4	4.8	337.4	8.4	257.2	-17.4
0.63181	337.3	354.4	5.1	368.0	9.1	273.9	-18.8
0.65847	371.7	392.2	5.5	409.5	10.2	295.5	-20.5
0.68986	416.0	441.2	6.0	464.1	11.6	322.5	-22.5
0.71065	449.0	476.6	6.1	504.0	12.2	341.2	-24.0
0.72872	481.3	509.4	5.8	541.1	12.4	358.0	-25.6

* Experimental data taken from P. Malbrunot and B. Vodar, "Experimental pVT Data and Thermodynamic Properties of Nitrogen up to 1000°C and 5000 Bar," Physica, vol 66, 1973, p 351.

Table 13. Observed and calculated pressure of nitrogen at 500°C using the Lennard-Jones 6-12 intermolecular potential

Density (g/cm³)	Observed* (MPa)	Percus-Yevic (MPa)	Error (%)	Verlet-Weis (MPa)	Error (%)	Two virial coefficients (MPa)	Error (%)
				Calculated			
0.26306	82.5	83.88	1.7	83.98	1.8	81.87	-0.8
0.29259	97.15	97.77	0.6	97.95	0.8	94.63	-2.6
0.34255	124.5	124.4	0.0	124.87	0.3	118.3	-5.0
0.3715	142.0	142.0	0.0	142.69	0.4	133.4	-6.0
0.41637	171.85	172.7	0.5	174.09	1.3	158.8	-7.6
0.46767	210.6	213.9	1.6	216.7	2.9	191.0	-9.3
0.51182	248.73	255.6	2.8	260.2	4.6	221.8	-10.8
0.5313	267.3	276.0	3.2	281.8	5.4	236.2	-11.6
0.55406	290.7	301.6	3.7	309.0	6.3	253.9	-12.6
0.5721	310.8	323.3	4.0	332.3	6.9	268.5	-13.6
0.61041	359.1	373.9	4.1	386.9	7.7	301.3	-16.1
0.63209	390.0	405.5	4.0	421.4	8.0	321.0	-17.7
0.65854	430.0	447.2	4.0	467.3	8.7	346.2	-19.5
0.6901	480.2	502.0	4.5	528.2	10.0	377.8	-21.3

* Experimental data taken from P. Malbrunot and B. Vodar, "Experimental pVT Data and Thermodynamic Properties of Nitrogen up to 1000°C and 5000 Bar," Physica, vol 66, 1973, p 351.

26

Table 14. Observed and calculated pressure of nitrogen at 700°C
using the Lennard-Jones 6-12 intermolecular potential

		Calculated					
Density (g/cm³)	Observed* (MPa)	Percus-Yevic (MPa)	Error (%)	Verlet-Weis (MPa)	Error (%)	Two virial coefficients (MPa)	Error (%)
0.23976	94.8	94.2	-0.6	94.37	-0.4	92.71	-2.2
0.28552	123.0	120.4	-2.1	120.8	-1.8	117.3	-4.6
0.31924	145.6	142.2	-2.3	142.8	-1.9	137.3	-5.7
0.34213	161.9	158.4	-2.2	159.1	-1.7	151.7	-6.3
0.36997	182.85	179.6	-1.8	180.7	-1.2	170.3	-6.9
0.41611	220.6	219.0	-0.7	221.1	0.2	203.9	-7.6
0.46171	262.3	264.1	0.7	267.8	2.1	240.6	-8.3
0.49141	292.4	297.2	1.6	302.3	3.4	266.4	-8.9
0.53231	338.7	348.1	2.8	355.9	5.1	304.8	-10.0
0.56183	376.1	389.0	3.4	399.5	6.2	334.5	-11.1
0.58396	406.2	422.4	4.0	435.2	7.1	357.9	-11.9
0.60891	442.0	462.8	4.7	478.9	8.3	385.6	-12.8
0.63278	480.1	504.5	5.1	524.3	9.2	413.4	-13.9

* Experimental data taken from P. Malbrunot and B. Vodar, "Experimental pVT Data and Thermodynamic
Properties of Nitrogen up to 1000°C and 5000 Bar," Physica, vol 66, 1973, p 351.

Table 15. Observed and calculated pressure of nitrogen at 800°C using the Lennard-Jones 6-12 intermolecular potential

		Calculated					
Density (g/cm^3)	Observed* (MPa)	Percus-Yevic (MPa)	Error (%)	Verlet-Weis (MPa)	Error (%)	Two virial coefficients (MPa)	Error (%)
0.2037	84.25	82.94	-1.5	84.14	-0.1	83.25	-1.2
0.2484	111.55	109.51	-1.8	109.72	-1.6	107.72	-3.4
0.2863	137.62	133.86	-2.7	134.25	-2.4	130.6	-5.1
0.3196	162.65	157.64	-3.1	158.30	-2.7	152.5	-6.2
0.3414	180.0	174.56	-3.0	175.4	-2.6	167.8	-6.8
0.3800	212.4	207.4	-2.4	208.9	-1.6	196.8	-7.3
0.4152	243.7	240.9	-1.1	243.3	-0.2	225.5	-7.5
0.4621	289.2	291.6	-0.8	295.8	2.3	267.3	-7.6
0.4917	321.2	327.6	2.0	333.3	3.8	296.0	-7.8
0.5194	354.6	364.4	2.8	372.0	4.9	324.4	-8.5
0.5343	374.1	385.5	3.0	394.3	5.4	340.4	-9.0
0.5601	410.0	424.4	3.5	435.7	6.3	369.2	-10.0
0.5833	443.3	462.1	4.2	476.1	7.4	396.4	-10.6
0.6099	485.3	508.8	4.8	526.5	8.5	429.1	-11.6

* Experimental data taken from P. Malbrunot and B. Vodar, "Experimental pVT Data and Thermodynamic Properties of Nitrogen up to 1000°C and 5000 Bar," Physica, vol 66, 1973, p 351.

Table 16. Observed and calculated pressure of nitrogen at 900°C using the Lennard-Jones 6-12 intermolecular potential

Density (g/cm³)	Observed* (MPa)	Calculated					
		Percus-Yevic (MPa)	Error (%)	Verlet-Weis (MPa)	Error (%)	Two virial coefficients (MPa)	Error (%)
0.2009	92.3	90.5	-2.0	89.43	-3.1	89.74	-2.8
0.2521	126.64	122.52	-3.2	122.78	-3.0	120.56	-4.8
0.2863	153.0	146.7	-4.1	147.2	-3.8	143.4	-6.3
0.3177	179.1	171.1	-4.5	171.9	-4.0	166.0	-7.3
0.3400	198.3	189.9	-4.2	190.9	-3.7	183.1	-7.7
0.3798	233.7	226.7	-2.0	228.4	-7.3	215.9	-7.6
0.4161	267.5	264.3	-1.2	267.0	-0.2	248.4	-7.1
0.4372	288.4	288.2	-0.1	291.7	1.2	268.5	-6.9
0.4630	315.8	319.5	1.2	324.1	2.6	294.4	-6.8
0.4915	349.4	357.0	2.2	363.3	3.9	324.6	-7.1
0.5090	372.2	381.7	2.6	389.2	4.6	344.1	-7.5
0.5334	406.2	418.4	3.0	427.9	5.3	372.5	-8.3
0.5606	444.6	462.5	4.0	474.9	6.8	405.8	-8.7
0.5854	481.7	506.0	5.0	521.5	8.3	437.7	-9.1

* Experimental data taken from P. Malbrunot and B. Vodar, "Experimental pVT Data and Thermodynamic Properties of Nitrogen up to 1000°C and 5000 Bar," Physica, vol 66, 1973, p 351.

Table 17. Observed and calculated pressure of nitrogen at 1000°C using the Lennard-Jones 6-12 intermolecular potential

Density (g/cm³)	Observed* (MPa)	Calculated					
		Percus-Yevic (MPa)	Error (%)	Verlet-Weis (MPa)	Error (%)	Two virial coefficients (MPa)	Error (%)
0.1618	78.5	75.0	-4.4	74.08	-5.6	74.68	-4.8
0.1774	87.75	84.04	-4.2	84.12	-4.1	83.58	-4.8
0.2041	105.02	100.44	-4.4	100.58	-4.2	99.61	-5.2
0.2439	134.07	127.28	-5.1	127.55	-4.9	125.54	-6.4
0.3173	196.06	185.56	-5.3	186.39	-4.9	180.34	-8.0
0.3407	217.2	206.9	-4.7	208.1	-4.2	199.9	-8.0
0.3803	254.03	246.6	-3.0	248.5	-2.3	235.4	-7.4
0.4172	291.1	287.9	-1.1	291.0	0.0	271.4	-6.8
0.4374	312.75	312.6	0.0	316.4	1.2	292.4	-6.5
0.4613	340.3	343.7	1.0	348.7	2.5	318.4	-6.4
0.4905	377.4	384.8	2.0	391.6	3.8	352.0	-6.7
0.5076	400.7	410.6	2.4	418.6	4.5	372.7	-7.0
0.5351	439.2	454.9	3.6	465.4	6.0	407.4	-7.2
0.5628	480.3	503.3	4.8	516.8	7.6	444.3	-7.5

* Experimental data taken from P. Malbrunot and B. Vodar, "Experimental pVT Data and Thermodynamic Properties of Nitrogen up to 1000°C and 5000 Bar," Physica, vol 66, 1973, p 351.

30

Table 18. Calculation of nitrogen pressure at T = 3000 K

Density (g/cm^3)	Observed* (KPa)	Calculated					
		Percus-Yevic (KPa)	Error (%)	Verlet-Weis (KPa)	Error (%)	Two virial coefficients (KPa)	Error (%)
0.1618	181.7	179.5	-1.2	176.8	-2.7	176.2	-3.0
0.1774	203.6	201.1	-1.2	197.9	-2.8	197.0	-3.2
0.2041	243.2	240.3	-1.2	236.1	-2.9	234.7	-3.5
0.2439	307.4	303.8	-1.2	298.1	-3.0	295.1	-4.0
0.3173	444.4	432.6	-2.6	430.6	-3.1	421.8	-5.1
0.3407	493.7	485.9	-1.6	478.6	-3.0	466.7	-5.5
0.3803	584.1	572.9	-1.9	566.7	-3.0	547.8	-6.2

* Extrapolated pressure using the hard-sphere equation of state.

31

Table 19. Fit of Lennard-Jones 6-12 potential to nitrogen
pressure data using Verlet-Weis theory

Temperature (°C)	σ (nm)	ε/k (K)	Largest error (%)
200	0.36202	87.10	2.0
300	0.36212	75.39	1.2
400	0.36275	74.51	0.6
500	0.36406	75.36	1.4
700	0.38228	21.37	1.8
800	0.38337	21.35	2.1
900	0.38536	20.91	3.5
1000	0.38808	21.00	4.0

DISTRIBUTION LIST

Commander
U.S. Army Armament Research and
  Development Command
ATTN: DRDAR-GCL
       DRDAR-LC, J. Frasier
       DRDAR-LCA, H. Fair
       DRDAR-LCA-G, D. Downs
       DRDAR-LCA-G, L. Harris
       DRDAR-LCE, R. Walker
       DRDAR-LCE, J. P. Picard
       DRDAR-SC, L. Stiefel
       DRDAR-TSS (5)
Dover, NJ 07801

Chief
Benet Weapons Laboratory, LCWSL
U.S. Army Armament Research and
  Development Command
ATTN: DRDAR-LCB-TL
Watervliet, NY 12189

Director
U.S. Army TRADOC Systems
  Analysis Activity
ATTN: ATAA-SL
White Sands Missile Range NM 88002

Director
U.S. Army Materials and Mechanics
  Research Center
ATTN: J. W. Johnson
Watertown, MA 02172

Director
U.S. Army Research Office
P.O. Box 12211
Research Triangle Park, NC 27709

Commander
U.S. Naval Surface Weapons Center
Dahlgren, VA 22448

Commander
U.S. Naval Ordnance Station
Indian Head, MD 20640

Director
U.S. Army Materiel Systems
  Analysis Activity
ATTN: DRXSY-MP
Aberdeen Proving Ground, MD 21005

Director
Ballistics Research Laboratory
U.S. Army Armament Research and
  Development Command
ATTN: DRDAR-TSB-S
       DRDAR-BL
       DRDAR-BLP, L. Watermeier
       DRDAR-BLP, J. M. Frankle
       DRDAR-BLP, E. Freedman
Aberdeen Proving Ground, MD 21005

Administrator
Defense Technical Information Center
ATTN: Accessions Division (12)
Cameron Station
Alexandria, VA 22314

Director of Defense Research
  and Engineering
ATTN: R. Thorkildsen
The Pentagon
Arlington, VA 20301

Defense Advanced Research
  Projects Agency
Director, Materials Division
1400 Wilson Boulevard
Arlington, VA 22209

Commander
U.S. Army Materiel Development and
  Readiness Command
ATTN: DRCDMD-ST
5001 Eisenhower Avenue
Alexandria, VA 22333

Commander/Director
Chemical Systems Laboratory
U.S. Army Armament Research and
  Development Command
ATTN: DRDAR-CLJ-L
       DRDAR-CLB-PA
APG, Edgewood Area, MD 21010

Commander
U.S. Army Armament Materiel
 Readiness Command
ATTN: DRSAR-LEP-L
Rock Island, IL 61299